DIMETHYL *N*-CYANODITHIOIMINOCARBONATE AND TRIPHENYLPHOSPHINE OXIDE METAL HALIDE COMPLEXES: MOLECULAR CRYSTAL ELUCIDATION

MOUHAMADOU BIRAME DIOP*[1], MODOU SARR[1], SERIGNE CISSE[1], LIBASSE DIOP[1], ALLEN G. OLIVER[2], DAVID HUGHES[3]

[1]*Inorganic and Analytical Chemistry Laboratory, Department of Chemistry, Faculty of Science and Technology, Cheikh Anta Diop University,Dakar, Senegal*

[2]*Department of Chemistry and Biochemistry, University of Notre Dame, Nieuwland, Science Hall, Notre Dame, USA*

[3]*School of Chemistry, University of East Anglia, Norwich, UK*

Abstract: Two MX_2 (M = Ni, Zn; X = Cl, Br) dimethyl *N*-cyanodithioiminocarbonate compounds and one $CrCl_2$ triphenylphosphine oxide complex were isolated and elucidated by single crystal X-ray crystallography. $NiCl_2[(CH_3S)_2C{=}NC{\equiv}N]_2$ (**1**) features inversion-related hydrogen bonded dimers linked into chains interacting through C–H···Cl growing layers along [110] whose junction into a 3D structure is enabled by H-bonds. $ZnBr_2[(CH_3S)_2C{=}NC{\equiv}N]_2$ (**2**) also exhibits inversion-related H-bonded dimers. In contrast with **1**, the structure of **2** comprises chains along [110], connected *via* C–H···Br and C–H···S into a 2D layer along [-110]. $CrCl_2(OPPh_3)_2$ (**3**) obtaining undergone redox processes, oxidizing $[CH_3C(O)CH_2PPh_3]^+$ to form PPh_3PO, and reducing Cr from Cr^{VI} to Cr^{II}. In the structure, each molecule is linked to height neighbors through H-bonds affording a 3D network.

Keywords: crystal, dimethyl *N*-cyanodithioiminocarbonate, Ni(II), Zn(II), Cr(II), redox process, 2D-structure, 3D-structure

1. INTRODUCTION

Dimethyl *N*-cyanodithioiminocarbonate crystal structures investigations are so far uncommon. Apart crystal structures of Co^{II} and Zn^{II} chloride, and triphenyltin(IV) we earlier reported [1–3], only one crystal compound of Cu^{I} chloride has been reported in 1992, by another group [4]. Few investigations report the use of dimethyl *N*-cyanodithioiminocarbonate as precursor for the isolation of pyrimidines derivatives holding antioxidant properties, and quinazolinone derivatives [5, 6]. Our previous works exhibited dimethyl *N*-cyanodithioiminocarbonate to merely behave as a N-donor ligand, in the solid state, coordinating metal atoms, though containing several basic sites [1–3]. Moreover, the ligand disconnects to metal centers, in solution; this might be the main difficulty to its coordinating investigation towards metallic centers in solution [3].

Related ligands *viz* cyanoimidodithiocarbonate aroused interest because of the multiple physical properties they exhibit. Indeed, the application of ruthenium bipyridyl cyanoimidodithiocarbonate in dye-sensitized solar cells,

* Corresponding author, email: mouhamadoubdiop@gmail.com

the magnetic and conducting properties were investigated [7-9]. The cyanoimidodithiocarbonate ligands adopt a general S, S-bidentate bridging or chelating coordination fashion [7-10].

In a former attempt to widen data on the coordination ability of this N-donor ligand, dimethyl *N*-cyanodithioiminocarbonate has surprisingly undergone redox reactivity at both the cyanide and the imido functionalities, in the presence of chromyl chloride, CrO_2Cl_2 [11]. Acetonyltriphenylphosphonium can be used as a counter ion to stabilize an anion but may be an O-donor ligand coordinating to metal centers with its oxygen O atom. Very few crystalline compounds relating to acetonyltriphenylphosphonium have been encountered in the literature [12–15].

Continuing our attempts to broaden data on the coordination ability of these two species *viz* dimethyl *N*-cyanodithioiminocarbonate and acetonyltriphenylphosphonium ion, whose crystal structures are merely scarce, we have investigated the reactions in solution media, of dimethyl *N*-cyanodithioiminocarbonate with nickel(II) chloride hexahydrate or zinc(II) bromide, and acetonyltriphenylphosphonium chloride, $CH_3C(O)CH_2PPh_3Cl$ with chromyl chloride, CrO_2Cl_2: this has afforded single crystals of $NiCl_2[(CH_3S)_2C{=}NC{\equiv}N]_2$ (**1**), $ZnBr_2[(CH_3S)_2C{=}NC{\equiv}N]_2$ (**2**) and $CrCl_2(OPPh_3)_2$ (**3**), for which crystallographic X-ray analyses have been carried out and reported in this work.

2. EXPERIMENTAL SETUP

2.1. General

All chemicals were purchased from Sigma-Aldrich, Germany and were used without any further purification. The X-ray crystallographic data for **1**, **2** and **3** were collected using a Bruker Kappa X8-APEX-II diffractometer working at 120 K, a Bruker APEX-II DUO diffractometer working at 100 K and an Oxford Diffraction Xcalibur 3/Sapphire3 CCD working at 140 K, respectively.

2.2. Synthesis of $NiCl_2[(CH_3S)_2C{=}NC{\equiv}N]_2$ (1)

The isolation of **1** occurred by mixing nickel(II) chloride hexahydrate ($NiCl_2.6H_2O$) [0.4136 g (1.740 mmol)] in 25 mL of a methanol/acetonitrile (3:2 mixture) and dimethyl *N*-cyanodithioiminocarbonate, $(CH_3S)_2C{=}NC{\equiv}N$ [0.2545 g (1.740 mmol)] in 15 mL of acetonitrile. The resulting clear solution is subsequently stirred 2h. A greenish powder was collected.

Recrystallization of an amount of the greenish powder in 25 mL of acetone afforded colorless plate-like crystals suitable for a single-crystal X-ray diffraction analysis, after some days of slow solvent evaporation at room temperature (305 K) and finally characterized as **1**.

2.3. Synthesis of $ZnBr_2[(CH_3S)_2C{=}NC{\equiv}N]_2$ (2)

The isolation of **2** occurred by mixing zinc(II) bromide ($ZnBr_2$) [0.3446 g (1.530 mmol)] in 15 mL of acetonitrile and dimethyl *N*-cyanodithioiminocarbonate, $(CH_3S)_2C{=}NC{\equiv}N$ [0.2238 g (1.530 mmol)] in 15 mL of acetonitrile. The resulting clear solution is subsequently stirred 2h. Colorless block-like crystals suitable for a single-crystal X-ray diffraction study were obtained, after some days of slow solvent evaporation at room temperature (305 K) and characterized as **2**.

2.4. Synthesis of $CrCl_2(OPPh_3)_2$ (3)

The isolation of **3** occurred by mixing chromyl chloride (CrO_2Cl_2) [0.4338 g (2.800 mmol)] in 25 mL of acetonitrile and acetonyltriphenylphosphonium chloride, $CH_3C(O)CH_2PPh_3Cl$ [0.4968 g (1.400 mmol)] in 25 mL of acetonitrile. The clear solution that is obtained is subsequently stirred 2h. Colorless block-like crystals suitable for a single-crystal X-ray diffraction study were obtained, after some days of slow solvent evaporation at room temperature (305 K) and characterized as **3**.

The proposed equations of reactions leading to the isolation of compounds **1**, **2** and **3** are shown as follow:

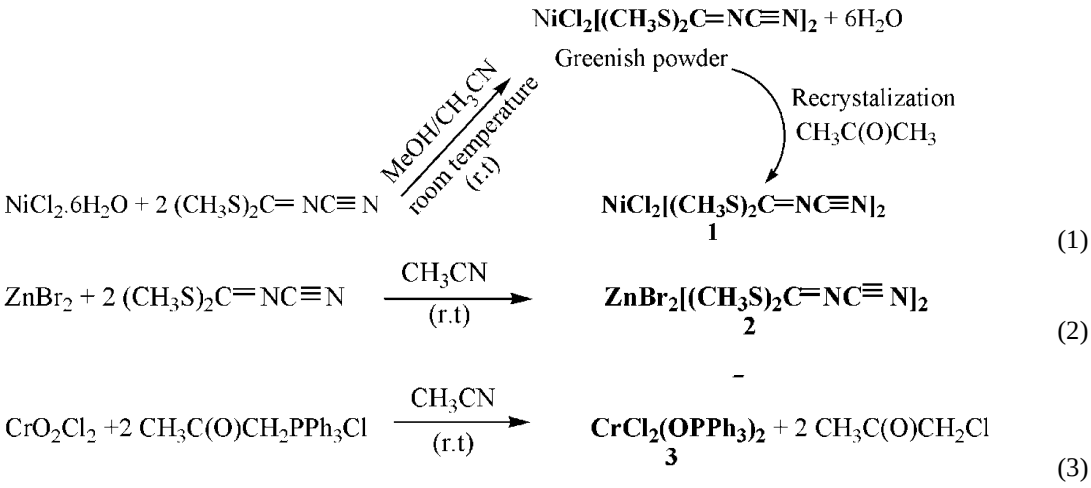

2.5. X-ray crystallography

The X-ray crystallographic data for compound **1** were collected using a Bruker Kappa X8-APEX-II diffractometer at T = 120 (2) K. Data were measured using φ and ω scans using MoKα radiation (λ = 0.71073 Å) using a collection strategy to obtain a hemisphere of unique data determined by Apex3 [16]. Cell parameters were determined and refined using the SAINT program [17]. Data for **1** were corrected for absorption and polarization effects and analyzed for space group determination [18]. The structure was solved by dual-space analysis using SHELXT [19] and the structure refined using least-squares minimization (SHELXL) [20]. The X-ray crystallographic data for **2** were collected at T = 100 (2) K using a Bruker DUO diffractometer using MoKα radiation (λ = 0.71073 Å) and an APEXII CCD area detector. Data were measured using φ and ω scans using MoKα radiation using a collection strategy to obtain a hemisphere of unique data determined by Apex2 [21]. Cell parameters were determined and refined using the SAINT program [17]. Data for **2** were corrected for absorption and polarization effects using intensity measurements by SADABS [22]. The structure was solved by dual-space analysis using SHELXT [19] and the structure refined using least-squares minimization (SHELXL) [20]. The X-ray crystallographic data for **3** were collected using an Oxford Diffraction Xcalibur 3/Sapphire3 CCD using MoKα radiation (λ = 0.71073 Å) operating at T = 140 (9) K. Data were measured using φ and ω scans using MoKα (λ = 0.71073 Å) radiation using a collection strategy to obtain a hemisphere of unique data determined by CrysAlisPro (Version 1.171.37.35) [23]. Cell parameters were determined and refined using the CrysAlisPro version 1.171.37.35) [23]. Data for **2** were corrected for absorption and polarization effects by CrysAlisPro (Version 1.171.37.35) empirical absorption correction using spherical harmonics, implemented in SCALE3 ABSPACK scaling algorithm [23]. The structure was solved by the direct method using SHELXS [24] and the structure refined using least-squares minimization (SHELXL) [20].

Programs used for the representation of the molecular and crystal structures: Olex2 [25] and Mercury [26]. The Crystallographic data and experimental details for structural analyses of compounds **1**, **2** and **3** are summarized in Table 1. Selected bond lengths and angles for **1**, **2** and **3** are listed in Tables 2 and 3.

CCDC 2057848 (**1**), 2057849 (**2**) and 2057850 (**3**) contain the supplementary crystallographic data for this paper. Copies of these data can be obtained free of charge from the Cambridge Crystallographic Data Center, 12 Union Road, Cambridge CB2 1EZ, UK (fax: int. Code +44 1223 336 033 *via* www.ccdc.cam.ac.uk/data_request/cif).

Table 1. Crystal data and structure refinement for compounds (**1**), (**2**) and (**3**).

Parameters	**Compound**		
	1	**2**	**3**
Empirical formula	$C_8H_{12}Br_2N_4S_4Zn$	$C_8H_{12}Cl_2N_4NiS_4$	$C_{36}H_{30}Cl_2CrO_2P_2$
Formula weight	517.65	422.07	679.44
Temperature (K)	100 (2)	120 (2)	140.0 (9)
Crystal system	Triclinic	Triclinic	Orthorhombic
Space group	*P-1*	*P-1*	*Fdd2*
a, (Å)	9.0562 (7)	8.8753 (5)	32.5690 (13)
α, (°)	71.2503 (13)	73.151 (3)	90

b, (Å)	9.0748 (7)	8.8935 (5)	20.8910 (7)
β, (°)	86.2376 (14)	87.437 (3)	90
c, (Å)	11.5415 (9)	11.2505 (7)	9.7440 (3)
γ, (°)	79.3252 (14)	79.952 (3)	90
Volume (Å^3)	882.62 (12)	836.86(9)	6629.8 (4)
Z	2	2	8
ρ_{calc} (g/cm^3)	1.948	1.523	1.361
μ (mm^{-1})	6.382	1.967	0.634
F(000)	504	428	2800
Crystal size (mm^3)	0.087 × 0.025 × 0.025	0.348 × 0.110 × 0.068	0.37 × 0.18 × 0.15
Radiation (Å)	MoKα (λ = 0.71073)	MoKα (λ = 0.71073)	MoKα (λ = 0.71073)
2Θ range for data collection (°)	1.863–27.496	1.891–28.372	3.650–27.493
Index ranges	-11 ≤ *h* ≤ 11	- 11≤ *h* ≤ 11	- 42≤ *h* ≤ 42
	- 11 ≤ *k* ≤ 11	- 11 ≤ *k* ≤ 11,	- 27 ≤ *k* ≤ 27,
	- 14 ≤ *l* ≤ 14	- 15 ≤ *l* ≤ 15	- 12 ≤ *l* ≤ 12
Reflections collected	19154	17216	26324
Independent reflections	4046[R_{int} = 0.0333]	4172 [R_{int} = 0.0259]	3798[R_{int} = 0.0331]
Data/restraints/parameters	4046/120/176	4172/0/176	3798/1/195
Goodness-of-fit on F^2	1.034	1.049	1.115
Final R indexes	R_1 = 0.0236,	R_1 = 0.0327,	R_1 = 0.0239,
[*I*> 2σ(*I*)]	wR_2 = 0.0490	wR_2 = 0.0832	wR_2 = 0.0587
Final R indexes	R_1 = 0.0353,	R_1 = 0.0395,	R_1 = 0.0243,
[all data]	wR_2 = 0.0524	*w*R_2 = 0.0865	*w*R_2 = 0.0589
Largest diff. peak/hole (e Å^{-3})	0.799/–0.391	1.168/–0.505	0.277/–0.265

[a] $R1 = \Sigma(||F_o|-|F_c||)/\Sigma|F_o|$; [b] $wR2 = [\Sigma w(F_o^2-F_c^2)^2/\Sigma[w(F_o^2)^2]^{1/2}$ where $w = 1/[\sigma^2(F_o^2)+(0.0274P)^2+0.0666P]$ for **1**, $w = 1/[\sigma^2(F_o^2)+(0.0442P)^2+1.1016P]$ for **2** and $w = 1/[\sigma^2(F_o^2)+(0.0273P)^2+6.6320P]$ for **3** where $P = (F_o^2)+2F_c^2)/3$; [c] goodness of fit = $[\Sigma w(F_o^2-F_c^2)^2/(N_o-N_v)]^{1/2}$.

Table 2. Selected bond lengths (Å) and angles (°) for compounds **1** and **2.**

Compound **1**			
Atom–Atom	Distance	Atom–Atom	Distance
Ni1−N1	2.002 (2)	N4−C6	1.312 (3)
Ni1−N3	2.002 (2)	S1−C2	1.722 (3)
Ni1−Cl2	2.2066 (7)	S1−C3	1.795 (3)
Ni1−Cl1	2.2262 (7)	S2−C2	1.717 (2)
N1−C1	1.146 (3)	S2−C4	1.796 (3)
N2−C1	1.310 (3)	S3−C6	1.727 (2)
N2−C2	1.317 (3)	S3−C7	1.800 (3)
N3−C5	1.147 (3)	S4−C6	1.711 (2)
N4−C5	1.310 (3)	S4−C8	1.797 (3)
Atom-atom-atom	Angle value	Atom-atom-atom	Angle value
N1−Ni1−N3	106.76 (10)	N1−C1−N2	172.7 (3)
N1−Ni1−Cl2	110.58 (7)	C5−N4−C6	120.4 (2)
N3−Ni1−Cl2	108.83 (7)	N2−C2−S2	119.64 (19)
N1−Ni1−Cl1	106.72 (7)	N2−C2−S1	121.49 (19)
N3−Ni1−Cl1	106.94 (7)	S2−C2−S1	118.86 (14)
Cl2−Ni1−Cl1	116.54 (3)	N4−C6−S4	119.94 (19)
C1−N1−Ni1	166.4 (2)	N4−C6−S3	121.48 (19)
C5−N3−Ni1	167.1 (2)	S4−C6−S3	118.58 (14)
C1−N2−C2	120.2 (2)		
Compound **2**			
Atom–Atom	Atom–Atom	Atom–Atom	Atom–Atom
Zn1−N1	2.011 (2)	C4−S5	1.715 (2)
Zn1−N11	2.013 (2)	C4−S7	1.738 (2)
Zn1−Br2	2.3510 (4)	S5−C6	1.806 (2)
Zn1−Br1	2.3730 (4)	S7−C8	1.806 (2)

N1−C2	1.153 (3)	C14−S15	1.725 (2)
C2−N3	1.320 (3)	C14−S17	1.730 (2)
N3−C4	1.322 (3)	S15−C16	1.810 (2)
N11−C12	1.153 (3)	S17−C18	1.805 (2)
C12−N13	1.315 (3)	Atom-atom-atom	Atom-atom-atom
Atom-atom-atom	Atom-atom-atom	N1−C2−N3	172.5 (3)
N1−Zn1−N11	107.26 (9)	C2−N3−C4	120.4 (2)
N1−Zn1−Br2	109.78 (6)	N3−C4−S5	120.11 (18)
N11−Zn1−Br2	109.72 (6)	N3−C4−S7	121.06 (18)
N1−Zn1−Br1	106.36 (6)	N11−C12−N13	173.3 (3)
N11−Zn1−Br1	107.36 (6)	C12−N13−C14	119.9 (2)
Br2−Zn1−Br1	115.973 (15)	N13−C14−S15	119.84 (18)
C2−N1−Zn1	167.2 (2)	N13−C14−S17	121.24 (18)
C12−N11−Zn1	165.4 (2)	S15−C14−S17	118.91 (13)
N13−C14	1.323 (3)		

Table 3. Selected bond lengths (Å) and angles (°) for compound **3** [Symmetry code: (i) −*x*+1, −*y*+1, *z*].

Compound **3**			
Atom–Atom	Distance	Atom–Atom	Distance
Cr−O	2.0417 (17)	O−P	1.5048 (17)
Cr−O^{i}	2.0417 (17)	P−C31	1.793 (3)
Cr−Cl	2.3113 (7)	P−C21	1.794 (2)
Cr−Cl^{i}	2.3114 (7)	P−C11	1.796 (3)
Atom-atom-atom	Angle value	Atom-atom-atom	Angle value
O−Cr−O^{i}	98.12 (11)	O−P−C31	108.64 (11)
O−Cr−Cl	108.74 (6)	O−P−C21	112.78 (11)
O^{i}−Cr−Cl	112.39 (5)	C31−P−C21	107.60 (11)
O−Cr−Cl^{i}	112.39 (5)	O−P−C11	110.92 (11)
O^{i}−Cr−Cl^{i}	108.73 (6)	C31−P−C11	110.58 (11)
Cl−Cr−Cl^{i}	115.22 (4)	C21−P−C11	106.26 (11)
P−O−Cr	155.76 (12)		

3. RESULTS AND DISCUSSION

3.1. Crystal and molecular structure of compound 1

The complex **1** which crystallizes as colorless plate like-crystals in the triclinic space group P-1, comprises a Ni^{II} metal center coordinated to two chlorides and two cyanide nitrogen atoms from two N-donor dimethyl *N*-cyanodithioiminocarbonate ligands, to complete the tetrahedron like arrangement (Figure 1).

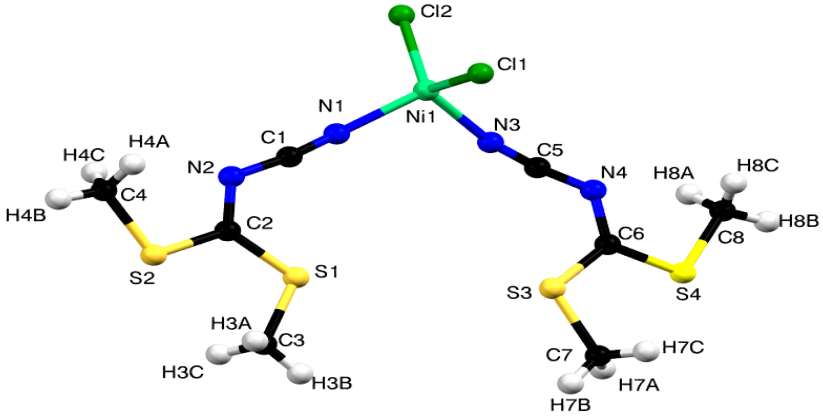

Fig. 1. Molecular view of compound **1** showing 50% probability ellipsoids for atoms and the crystallographic numbering scheme.

Ni–Cl and Ni−N bond lengths are within expected ranges (Table 2). The Cl−Ni−Cl angle is larger than an ideal tetrahedral angle while two of the Cl−Ni−N angles and the N−Ni−N angle are smaller and the two remaining Cl−Ni−N angle, slightly longer-smaller, are very close to the ideal tetrahedral angle. A weak distortion is incredibly encountered in this complex **1**, whereas *N*-cyanodithioiminocarbonate bulky ligands might strengthen the distortion [1, 2]. The nitrile groups within the N-donor ligands still hold triple-bond character, though the nitrogen atom is coordinated, in a bent fashion, to the Ni center, with C1≡N1 [1.146 (3) Å] and C5≡N3 [1.147 (3) Å]. The angular sums of the central C atoms of the ligands (360.0 and 359.99°) enforce the expected trigonal–planar geometry. The geometric parameters are in accordance with those found in the literature [1−4]. The dihedral angle of 5.60 (6)°, between the least-squares planes of the two dimethyl *N*-cyanodithioiminocarbonate ligands, indicates that these latter are almost co-planar. Within the structure positioning species, inversion-related pairs of complex molecules are featured. These pairs are arranged such that Cl1 is oriented between the methylthiol H_3C-S groups of the adjacent molecule: this presumably damp steric interaction [distances from closest S1 and S3 atoms: 5.9217 (6) and 6.0104 (10) Å, respectively]. Cl2 atom is oriented between methylthiol H_3C-S groups of two neighboring molecules from two different pairs so that distances between Cl2 and the two closest S2 and S4 are 8.2791 (11) and 8.1308 (10) Å, respectively (Figure 2).

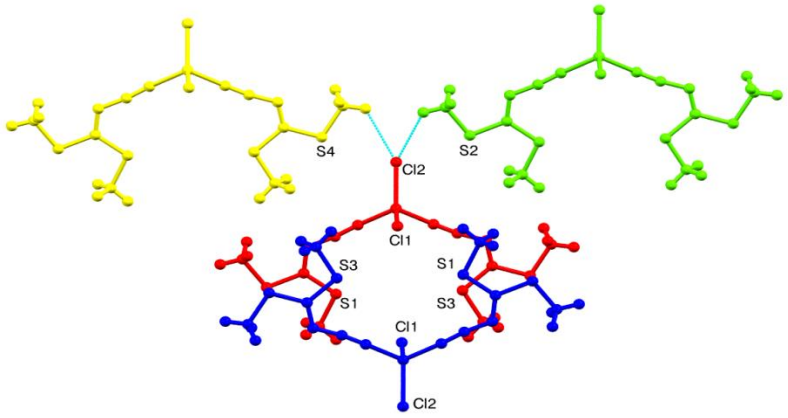

Fig. 2. Molecular view of **1** showing 50% probability ellipsoids for atoms, showing the positioning of molecules; one dimer in relation to two molecules from two different dimers (the second molecule within dimers, yellow and green colored, are omitted for clarity).

Inspection of the hydrogen bonding interactions exhibits that inversion-related pairs interact through C3–H3*B*···Cl1, C7–H7*B*···Cl1 and C4–H4*A*···S4 (see Figure 3 and Table 4 for details). The dimers are then connected by C4–H4*B*···Cl2 into infinite slabs parallel to [110] direction (see Figure 3 and Table 2 for details).

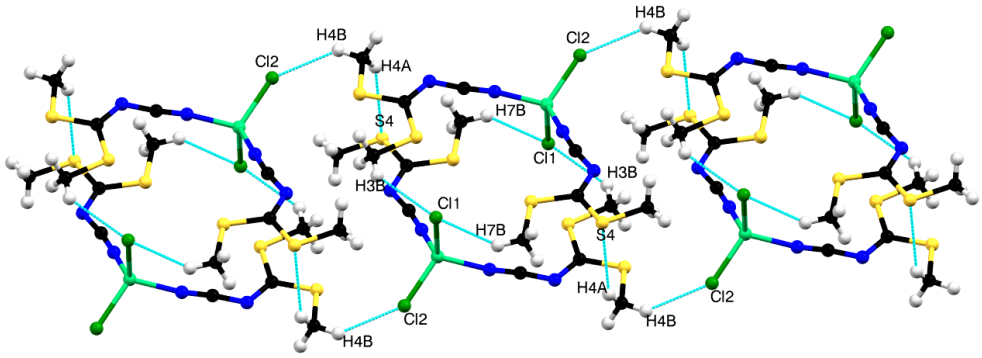

Fig. 3. Molecular view of **1** showing 50% probability ellipsoids for atoms, showing the interconnections between molecules forming dimers and the linkage of the dimers into infinite chain slabs.

In the structure, the infinite slabs are linked through interspecies C8–H8*B*···Cl2 hydrogen bonds, giving layers along [110] (see Figure 4 and Table 4 for details).

Contrary to the Zn and Co chloride homologues, in the complex **1**, the junction of the layers is enabled by C7–H7*A*···Cl2 hydrogen bonds, leading to the formation of a supramolecular three-dimensional structure (Figure 5 and Table 4). Thus, complex **1** is structurally different to its reported homologues reported before [1, 2].

3.2. Crystal and molecular structure of compound 2

The complex **2** crystallizes as colorless block like-crystals in the triclinic space group P-1. The asymmetric unit comprises a Zn^{II} metallic center coordinated by two bromides and two cyanide nitrogen atoms of two N-donor dimethyl *N*-cyanodithioiminocarbonate ligands (Figure 6).

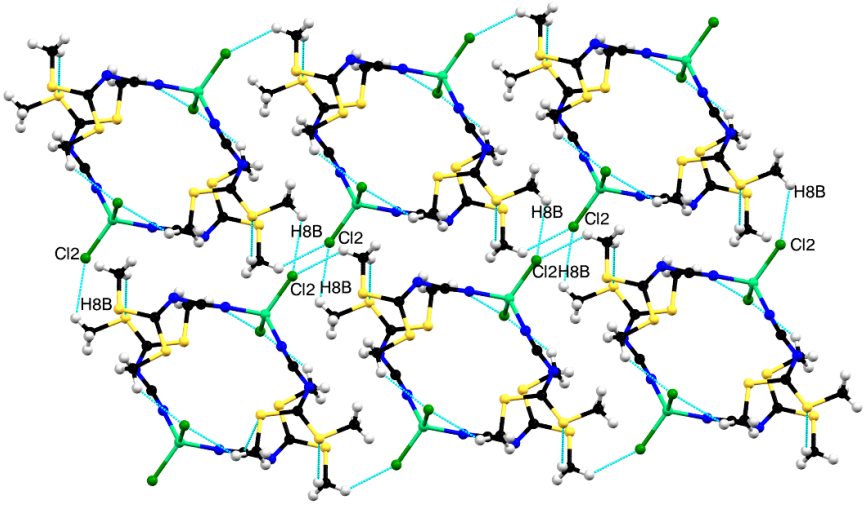

Fig. 4. Molecular view of **1** showing 50% probability ellipsoids for atoms, showing the layer along [110] formed through interconnections between the infinite chain slabs.

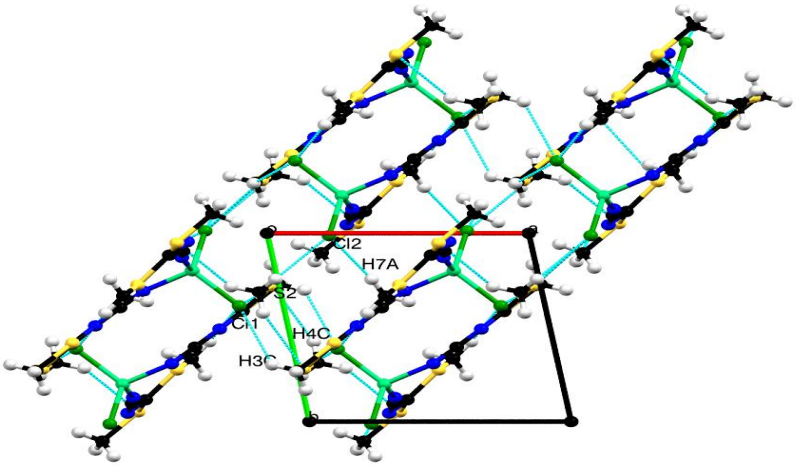

Fig. 5. Molecular view of **1** showing 50% probability ellipsoids for atoms, showing the 3D structure along [-110] plane afforded by hydrogen bonding interactions between layers lying down [110].

Table 4. Hydrogen bonds in crystals of **1** (Symmetry codes: (i) −*x*+1, −*y*+1, −*z*+1; (ii) *x*+1, *y*−1, *z*; (iii) −*x*+2, −*y*+1, −*z*; (iv) *x*+1, *y*, *z*; (v) −*x*+1, −*y*+2, −*z*+1; (vi) *x*, *y*, *z*+1)

D–H···*A*	*d*(*D*–H)	*d*(H···*A*)	*d*(*D*···*A*)	∠(*D*–H···*A*)
C4–H4A···S4^{i}	0.98	2.97	3.717 (3)	134
C4–H4B···Cl2^{ii}	0.98	2.73	3.453 (3)	131
C4–H4C···S2^{iii}	0.98	2.99	3.922 (3)	160
C3–H3B···Cl1^{i}	0.98	2.81	3.588 (3)	137

C3–H3C···Cl1^{iv}	0.98	2.89	3.589 (3)	130
C7–H7A···Cl2^{v}	0.98	2.74	3.720 (3)	175
C7–H7B···Cl1^{i}	0.98	2.85	3.599 (3)	134
C8–H8B···Cl2^{vi}	0.98	2.87	3.539 (3)	126

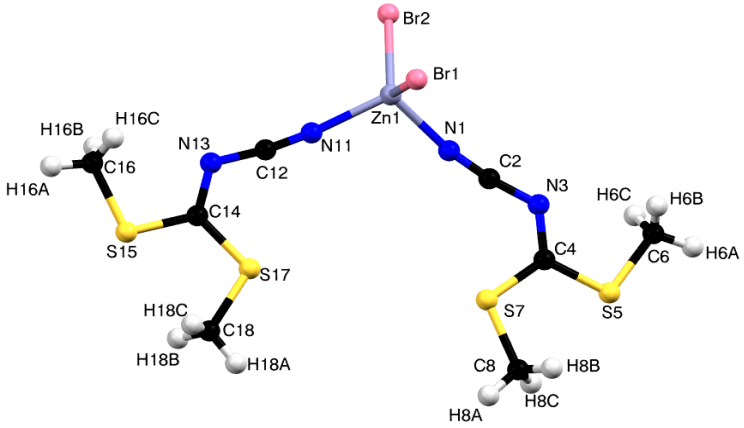

Fig. 6. Molecular view of **2** showing 50% probability ellipsoids for atoms and the crystallographic numbering scheme.

The Zn–Br and Zn−N bond lengths are in the expected ranges (Table 2). The Br−Zn−Br angle of 115.973 (15)°, larger than an ideal tetrahedral angle, is the major deviation. One of the Br−Zn−N angles and the N−Zn−N angle are smaller to the ideal tetrahedral angle, whereas the two other Br−Zn−N angles are very close to the ideal tetrahedral angle. While the bulkiness of the *N*-cyanodithioiminocarbonate ligands might strengthen the distortion, deviations are nevertheless weak as previously reported [1, 2]. The coordination of the ligand nitrile nitrogen atoms to Zn^{II} is bent and, the nitrile groups yet exhibit triple-bond character, although the coordination of the nitrogen atom to the Zn center; C2≡N1 [1.154 (3) Å] and C12≡N11 [1.153 (3) Å]. The sums of the angles at central C atoms of the ligands (360.0 and 359.99°) are in accordance with the expected trigonal–planar geometry. These parameters are comparable to those in **1**, and are in convenience with those found in the literature [1−4]. Contrary to compound **1**, present in this complex **2** is the positioning of the molecules. Indeed, the complex molecules are organized into inversion-related pairs. Thus, Br1 is oriented between the methylthiol H_3C−S groups of the adjacent molecule, presumably damping steric interactions [distances from closest S7 and S17 atoms: 6.0873(8) and 6.0391(8) Å, respectively]. Br2 atom is oriented between the methylthiol H_3C−S groups of two neighboring molecules from two different pairs such that separating distances between Br2 atom and the two closest S5 and S15 sulfur atoms are 8.2941 (9) and 8.3329 (10) Å, respectively (Figure 7).

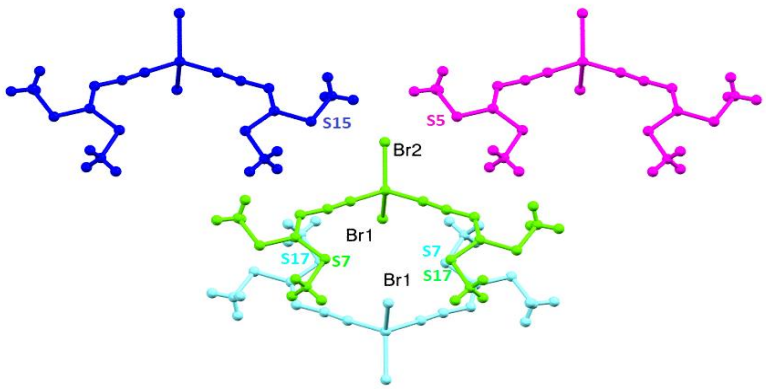

Fig. 7. Molecular view of **2** showing 50% probability ellipsoids for atoms, showing the positioning of molecules; one dimer in relation to two molecules from two different dimers (the second molecule within dimers, blue and purple colored, are omitted for clarity).

These values are the ranges of those found in **1**. The dihedral angle of 5.97 (6)°, between the least-squares planes of the two dimethyl *N*-cyanodithioiminocarbonate ligands, indicates a slight deviation from co-planarity. Close

inspection of hydrogen bonds exhibits that inversion-related pairs interact *via* C8–H8*A*···Br1 and C18–H18*A*···Br1 (Figure 8 and Table 5). Inversion-related dimers are connected by C16–16*A*···Br2 affording infinite slabs parallel to the [110] direction (Figure 8 and Table 5).

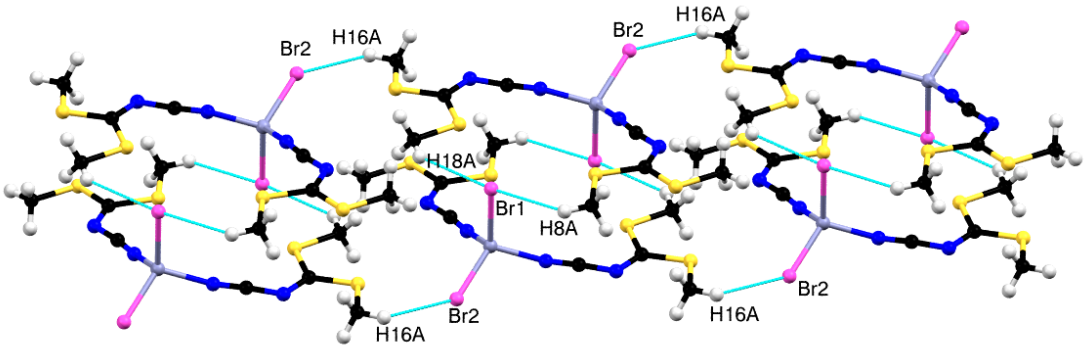

Fig. 8. Molecular view of **2** showing 50% probability ellipsoids for atoms, showing the interconnections between molecules forming dimers and the linkage of the dimers into infinite chain slabs.

In the structure, C8–H8*C*···Br2 and C16–H16*B*···S15 hydrogen bonds link the chains into a layer-like network (Figure 9), along [-110]. Owing to their involvement ratio in the hydrogen bonded assembly, almost a difference is not observed between Zn−Br1 2.3730 (4) Å and Zn−Br2 2.3510 (4) Å distances. In a structural point of view, the complex **2** is different to complex **1**, but is otherwise isomorphous and nearly isostructural to its chloride homologue we earlier published [1, 2].

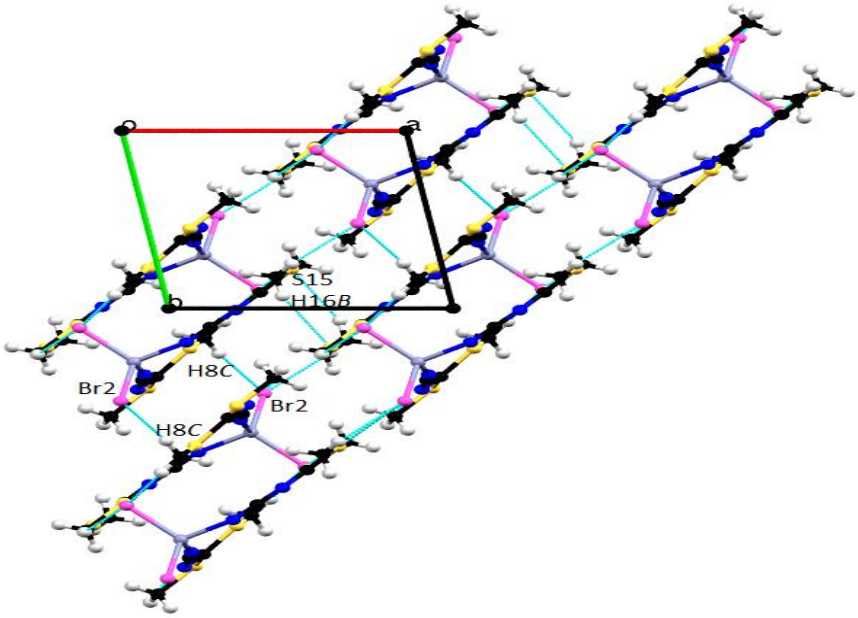

Fig. 9. Molecular view of **2** showing 50% probability ellipsoids for atoms, showing the layer along [-110] formed through interconnections between the infinite chain slabs.

Table 5. Hydrogen bonds in crystals of **2** (Symmetry codes: (i) −*x*, −*y*, −*z*+1; (ii) *x*+1, *y*−1, *z*; (iii) −*x*, −*y*+1, −*z*+1; (iv) −*x*+1, −*y*, −*z*)

D–H···*A*	*d*(*D*–H)	*d*(H···*A*)	*d*(*D*···*A*)	∠(*D*–H···*A*)
C8–H8A···Br1^{i}	0.98	2.99	3.724(3)	133
C8–H8C···Br2^{iii}	0.98	2.87	3.845(3)	172
C16–H16A···Br2^{ii}	0.98	2.92	3.622(2)	130
C16–H16B···S15^{iv}	0.98	2.97	3.910(3)	161
C18–H18A···Br1^{i}	0.98	2.97	3.724(3)	135

3.3. Crystal and molecular structure of compound 3

The complex **3** is the result of a redox process over the chrome complex used as starting material, when the reaction is undertaken in acetonitrile and in a non-controlled atmosphere. Indeed, the acetonyltriphenylphosphonium cation behaves as a reducing agent to reduce Cr^{VI} to Cr^{II}, and is at the same time oxidized forming triphenylphosphine oxide, $OPPh_3$. The methylene carbon atom of the acetonyl group linked to the phosphor atom, as the phosphor atom, has been oxidized and the phosphor atom bears an oxygen atom leading to the formation of the triphenylphosphine oxide, $OPPh_3$ molecule. Thus, removal of the acetonyl group has been observed during the unexpected reaction process; how the CrO_2Cl_2 and $CH_3C(O)CH_2PPh_3Cl$ play roles in this redox reaction is so far yet unknown. However, an inter-species reorganization happened (equation 3).

The complex **3** crystallizes as colorless block like-crystals in the orthorhombic space group F*dd2*. The asymmetric unit consists of Cr^{II} metal center coordinated to two chlorine atoms and two O atoms from two triphenylphosphine oxide ($OPPh_3$) molecules to complete the tetrahedron like-arrangement at chrome atom (Figure 10).

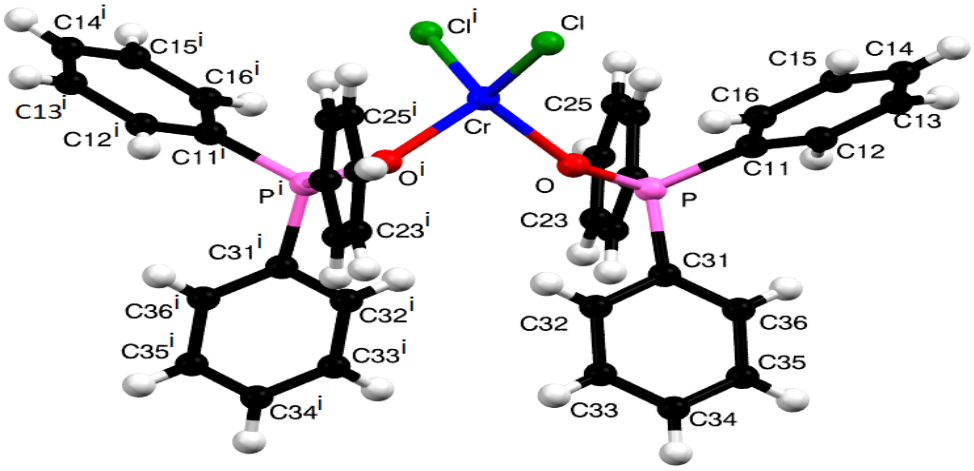

Fig. 10. Molecular view of **3** showing 50% probability ellipsoids for atoms and the crystallographic numbering scheme.

In the past, numerous transition metal crystalline compounds (Mn, Co, Ni, Cu, Zn, Cd; X = Cl, Br, I) of triphenylphosphine oxide, have been isolated and characterized using diverse techniques [27−35]. Almost all known $MX_2(OPPh_3)_2$ complexes have been isolated from reaction between metal halides and triphenylphosphine oxide, whereas only two examples undergone unexpected reactions, with in situ formation of $OPPh_3$ *viz* the reactions of the complex $[Mn(CH_3\text{-}\eta^5\text{-}(CO)_2PPh_3]$ with iodine [27], and 1-iodo-6-ptolylethynyl-2,3,4,5-tetraethyl-2,3,4,5-tetracarba-nido-hexaborane(6) with $ClZnC{\equiv}C(CH_2)_4C{\equiv}CZnCl$ in the presence of $Pd(PPh_3)_4$ [28]. In contrast to the general obtaining of $MX_2(OPPh_3)_2$, this compound **3**, the first chrome example, has been obtained from a different reaction route (equation 3). The coordination tetrahedron sphere is considerably distorted with angles varying from 98.12 (11) to 115.22 (6)°. The O-donor triphenylphosphine oxide ligand adopts a general position with bond and angle values in the expected ranges [27−35]. Cr−Cl lengths (Table 3) are not far from those observed for the chloride homologues reported in the literature [29−32]. In the structure, inter-species C–H···Cl hydrogen bonding interactions connect $CrCl_2(OPPh_3)_2$ molecules. Each $CrCl_2(OPPh_3)_2$ molecule is linked to eight neighbors (Figure 11 and Table 6). The expanded hydrogen bonding interactions between the molecules, give rise to a supramolecular three dimensional structure (Figure 11 and Table 6).

4. CONCLUSIONS

The salt **1** from inversion-related dimers exhibits infinite chains linked to give layers connected into a supramolecular hydrogen bonded three-dimensional network. In contrast, compound **2** describes inversion-related dimers whose expanded inter-species hydrogen bonding interactions give rise to a layer-like structure. The compound **3** is isolated from a non-common procedure; its formation evidences redox processes. A reduction is noted over the chromyl chloride complex while the acetonyltriphenylphosphonium cation undergoes

an oxidation; Cr^{VI} is reduced to Cr^{II} and in turn oxidized acetonyltriphenylphosphonium forming triphenylphosphine oxide. The interconnections between the molecules in **3** lead to the first hydrogen bonded $MX_2(PPh_3O)_2$, 3D-structure. Further works involving chromyl chloride and various organic reagents, with the aim of understanding the role of this former, are in progress.

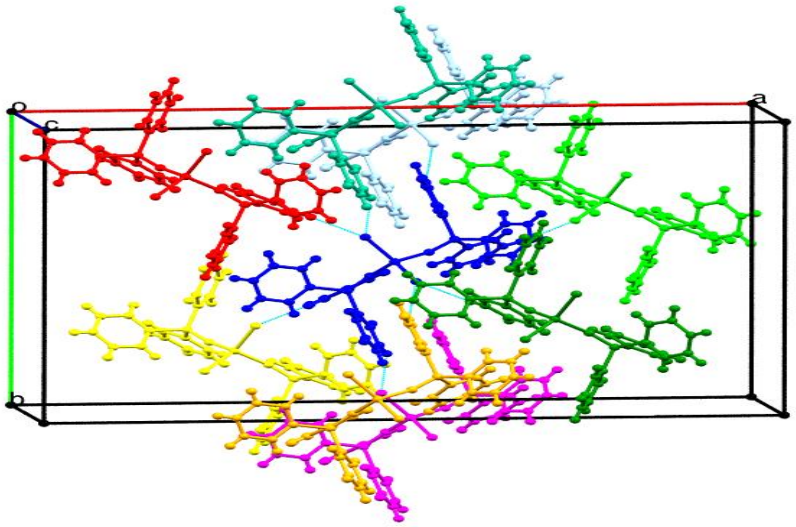

Fig. 11. Molecular view of **3** showing 50% probability ellipsoids for atoms, showing the 3D network grown from hydrogen bonding interactions between a molecule (blue) and its eight (8) neighbors (other colors).

Table 6. Hydrogen bonds in crystals of **3** (Symmetry codes: (i) −*x*+5/4, *y*−1/4, *z*−1/4; (ii) *x*, *y*−1/2, *z*+1/2; (iii) *x*, *y*, *z*+1; (iv) −*x*+5/4, *y*−1/4, *z*+3/4)

D–H···*A*	*d*(*D*–H)	*d*(H···*A*)	*d*(*D*···*A*)	∠(*D*–H···*A*)
C13−H13···O^{i}	0.93	2.95	3.759(3)	147
C16−H16···Cl	0.93	3.14	3.878(3)	138
C23−H23···Cl^{ii}	0.93	2.79	3.426(3)	127
C33−H33···Cl^{iii}	0.93	2.89	3.655(4)	140
C35−H35···Cl^{iv}	0.93	2.81	3.649(3)	151

ACKNOWLEDGEMENTS

The authors acknowledge the Cheikh Anta Diop University of Dakar (Senegal), the University of Notre Dame (USA), the National Science Foundation and the University of Florida (USA), and the University of East Anglia, Norwich (UK) for equipment facilities.

REFERENCES

[1] Diop, M.B., Diop, L., Oliver, A.G., Crystal structure of dichloridobis (dimethyl *N*-cyanodithioiminocarbonate) cobalt(II), Acta Crystallographica Section E, vol. 72, 2016, p. 66-68.
[2] Diop, M.B., Diop, L., Oliver, A.G., Crystal structure of dichloridobis (dimethyl *N*-cyanodithioiminocarbonate) zinc, Acta Crystallographica Section E, vol. 72, 2016, p. 417-419.
[3] Diop, M.B., Sow, Y., Diop, L., Plasseraud, L., Cattey, H., Crystal structure of the triphenyltin(IV) chloride dimethyl *N*-cyanodithioiminocarbonate adduct, Main Group Metal Chemistry, vol. 39, 2016, p. 113-117.
[4] Kojic-Prodic, B., Kiralj, R., Zlata, R., Sunjic, V., Promoting effect of copper ions in vinyl-like nucleophilic substitution in *N*-cyanoazomethines, analysis based on crystal structure data, Bulletin of the Slovenian Chemical Society, vol. 39, 1992, p. 367-381.
[5] Abuelizz, H.A., Taie, H.A.A., Marzouk, M., Al-Salahi, R., Synthesis and antioxidant activity of 2-methylthio-pyrido[3,2-*e*] [1, 2, 4] triazolo[1,5-*a*] pyrimidines, Open Chemistry, vol. 17, 2019, p. 823-830.

[6] Al-Salahi, R.A., Marzouk, M.S., Ghabbour, H.A., Kun, F.H., Synthesis of novel 2-(methylthio) benzo[g] [1,2,4] triazolo[1,5-a] quinazolin- 5-(4H)-one and its derivatives, Letters in Organic Chemistry, vol. 11, 2014, p. 759-767.
[7] McCall, K.L., Jennings, J.R., Wang, H., Morandeira, A., Peter, L.M., Durrant, J.R., Yellowlees, L.J., Woollins, J.D., Robertson, N., Novel ruthenium bipyridyl dyes with S-donor ligands and their application in dye-sensitized solar cells, Journal of Photochemistry and Photobiology A: Chemistry, vol. 202, no. 2-3, 2009, p. 196-204.
[8] Belo, D., Rodrigues, C., Santos, I.C., Silva, S., Eusébio, T., Lopes, E.B., Rodrigues, J.V., Matos, M.J., Almeida, M., Duarte, M.T., Henriques, R.T., Synthesis, crystal structure and magnetic properties of bis(3,4;3′,4′-ethylenedithio) 2,2′,5,5′-tetrathiafulvalene-bis (cyanoimidodithiocarbonate) aurate(III), (bedt-ttf) $[Au(cdc)_2]$, Polyhedron, vol. 25, no. 5, 2006, p. 1209-1214.
[9] Singh, N., Kumar, A., Organoheterobimetallic cyanodithioimidocarbonates and their I2-doped products: Synthesis, characterization and conducting properties, Synthetic Metals, vol. 158, 2008, p. 442-446.
[10] Burchell, C.J., Aucott, S.M., Milton, H.L., Slawin, A.M.Z., Derek Woollins, J., Synthesis and characterisation of cyanodithioimidocarbonate $[C_2N_2S_2]^{2-}$ complexes, Dalton Transactions, vol. 2004, no. 3, 2004, p. 369-374.
[11] Diop, M.B., Diop, L., Oliver, A.G., Crystal structure of *N*-[(methylsulfanyl)carbonyl]urea, Acta Crystallographica Section E, vol. 72, 2016, p. 325-327.
[12] Diop, M.B., Diop, L., Oliver, A.G., Acetonyltriphenylphosphonium 2,3,5-triphenyltetrazolium tetrachloridocuprate(II), Acta Crystallographica Section E, vol. 74, 2018, p. 69-71.
[13] Diop, M.B., Diop, L., Oliver, A.G., Crystal structure of bis(acetonyltriphenylphosphonium) tetrachloridocobaltate(II), Acta Crystallographica Section E, vol. 71, 2015, p. m209-m210.
[14] Diop, T., Diop, L., Kucerakova, M., Dusek, M., Acetonyltriphenylphosphonium nitrate, Acta Crystallographica Section E, 2013, vol. 69, p. o303.
[15] Szell, P.M.J., Gabidullin, B., Bryce, D.L., 1,3,5-Tri(iodoethynyl)-2,4,6-trifluorobenzene: halogen-bonded frameworks and NMR spectroscopic analysis, Acta Crystallographica Section B, vol. 73, 2017, p. 153-162.
[16] Apex3, Bruker AXS Inc., Madison, Wisconsin, USA, 2015.
[17] Saint, Area Detector Integration Software, Bruker AXS Inc., Madison, Wisconsin, USA, 2014.
[18] Krause, L., Herbst-Irmer, R., Sheldrick, G.M., Stalke, D., Comparison of silver and molybdenum microfocus X-ray sources for single-crystal structure determination, Journal of Applied Crystallography, vol. 48, 2015, p. 3-10.
[19] Sheldrick, G.M., *SHELXT* - Integrated space-group and crystal structure determination, Acta Crystallographica Section A, vol. 71, 2015, p. 3-8.
[20] Sheldrick, G.M., Crystal structure refinement with *SHELXL*, Acta Crystallographica Section C, vol. 71, 2015, p. 3-8.
[21] Apex2, Data Reduction and Frame Integration Program for the CCD Area-Detector System, Bruker AXS Inc., Madison, Wisconsin, USA, 2014.
[22] Blessing, R.H., An empirical correction for absorption anisotropy, Acta Crystallographica Section A, vol. 51, 1995, p. 33-38.
[23] CrysAlisPro (Version 1.171.37.35), Oxford Diffraction, Agilent Technologies UK Ltd, Yarnton, England.
[24] Sheldrick, G.M., A short history of *SHELX*, Acta Crystallographica Section A, vol. 64, 2008, p. 112-122.
[25] Dolomanov, O.V., Bourhis, L.J., Gildea, R.J., Howard, J.A.K., Puschmann, H., OLEX2: a complete structure solution, refinement and analysis program, Journal of Applied Crystallography, vol. 42, 2009, p. 339-341.
[26] Macrae, C.F., Bruno, I.J., Chisholm, J.A., Edgington, P.R., McCabe, P., Pidcock, E., Rodriguez-Monge, L., Taylor, R., van de Streek, J., Wood, P.A., Mercury CSD 2.0- new features for the visualization and investigation of crystal structures, Journal of Applied Crystallography, vol. 41, 2008, p. 466-470.
[27] Avilés, T., Carrondo, M.A.A.F. de C.T., Piedade, M.F.M., Teixeira, G., Reaction of $[Mn(CH_3\text{-}\eta^5\text{-}C_5H_4)(CO)_2PPh_3]$ with iodine. Crystal structure of diiodobis(triphenylphosphineoxide) manganese(II), Journal of Organometallic Chemistry, vol. 388, 1990, p. 143-149.
[28] Nie, Y., Pritzkow, H., Wadepohl, H., Siebert, W., Halogen exchange at boron in *nido*-C_4B_2 carboranes, Journal of Organometallic Chemistry, vol. 690, 2005, p. 4531-4536.
[29] Bertrand, J.A., Kalyanaraman, AR., The crystal and molecular structure of dichlorobis(triphenylphosphine oxide)copper(II), Inorganica Chimica Acta, vol. 5, 1971, p. 341-345.
[30] Kosky, C.A., Gayda, J.P., Gibson, J.F., Jones, S.F., Williams, D.J., Crystal Structures of dichlorobis (triphenylphosphine oxide) zinc(II) and dibromobis (triphenylphosphine oxide) zinc(II) and an EPR study of manganese(II) in dibromobis (triphenylphosphine oxide) zinc(II), Inorganic Chemistry, vol. 21, 1982, p. 3173-3179.

[31] Cotton, S.A., Franckevicius, V., Fawcett, J., Benchmark compounds. Structures of cobalt(II) complexes of triphenylphosphine- and triphenylarsine oxides, Transition Metal Chemistry, vol. 27, 2002, p. 38-41.
[32] Moreno-Fuquen, R., Cifuentes, O., Naranjo, J.V., Serratto, L.M., Kennedy, A.R., Dichlorobis (triphenylphosphine oxide-κO)nickel(II), Acta Crystallographica Section E, vol. 60, 2004, p. m1861-m1862.
[33] Shanthakumari, R., Hema, R., Ramamurthy, K., Stoeckli-Evans, H., Diiodidobis(triphenylphosphine oxide)-cadmium, Acta Crystallographica Section E, vol. 67, 2011, p. m114.
[34] Weinberger, P., Schamschule, R., Baumgartner, O., Linert, W., Structural and vibrational properties of dichlorobis (triphenylphosphineoxide) copper(ii), Journal of Coordination Chemistry, vol. 42, 1997, p. 171-180.
[35] Bertrand, J.A., Graham, S.L., Deutsch, H.M., van Derveer, D.G., The Crystal and Molecular Structure of Dibromobis(triphenylphosphine oxide)copper(II), Inorganica Chimica Acta, vol. 19, 1976, p. 189-193.